

# Evaluation of a pyroelectric detector with a carbon multiwalled nanotube black coating in the infrared

E. Theocharous, R. Deshpande, A. C. Dillon, and J. Lehman

The performance of a pyroelectric detector with a carbon multiwalled nanotube coating was evaluated in the 0.9–14  $\mu\text{m}$  wavelength range. The relative spectral responsivity of this detector was shown to be flat over most of the wavelength range examined, and the spectral flatness was shown to be comparable to the best infrared black coatings currently available. This finding is promising because black coatings with spectrally flat absorbance profiles are usually associated with the highest absorbance values. The performance of the detector (in terms of noise equivalent power and specific detectivity) was limited by the very thick (250  $\mu\text{m}$  thick)  $\text{LiNbO}_3$  pyroelectric crystal onto which the coating was deposited. The responsivity of this detector was shown to be linear in the 0.06–2.8 mW radiant power range, and its spatial uniformity was comparable to that of other pyroelectric detectors that use different types of black coating. The carbon nanotube coatings were reported to be much more durable than other infrared black coatings, such as metal blacks, that are commonly used to coat thermal detectors in the infrared. This, in combination with their excellent spectral flatness, suggests that carbon nanotube coatings appear extremely promising for thermal detection applications in the infrared. © 2006 Optical Society of America  
OCIS codes: 040.3060, 160.1890.

## 1. Introduction

Coatings applied to thermal detectors must combine high absorptivity, to ensure that a large fraction of the incident radiation is absorbed, with low thermal mass, to ensure that the resultant temperature increase is maximized for a certain level of incident radiant power.<sup>1</sup> These requirements are particularly important in the infrared, where there is limited availability of black coatings whose characteristics match the conditions stated above. While the absorptivities of gold-black coatings in the infrared are good,<sup>2,3</sup> the fibrous structure of these coatings is delicate, leading to degradation in performance owing to the collapse of this structure, particularly as a result of heating and physical contact. The physical properties of carbon nanotubes (CNTs) have been docu-

mented by CNT pioneers such as Saito *et al.*<sup>4</sup> Though different values may be reported in the literature for CNTs of various species and production methods, the evidence clearly indicates that CNT coatings have the advantages of mechanical strength, high melting temperature, and high thermal conductivity.<sup>4</sup> Lehman *et al.* recognized that the characteristics of CNT coatings fulfill the main requirements for black coatings for thermal detectors.<sup>5,6</sup> The fabrication and evaluation of two pyroelectric detectors with two different types of CNT coating were reported in the 600–1800 nm wavelength range.<sup>5,6</sup> However, the main applications of thermal detectors are in the infrared, where the advantages of alternative (photon) detector technologies are not so overwhelming, allowing thermal detectors to compete for market share. Our aim in this paper is to report the extension of the evaluation of a carbon multiwalled-nanotube-(MWNT-) coated pyroelectric detector in the infrared. The CNT coating, which was grown by hot-wire chemical-vapor deposition, was deposited onto a lithium niobate ( $\text{LiNbO}_3$ ) crystal<sup>5</sup> 250  $\mu\text{m}$  thick. The active area of the detector had a diameter of 3 mm. Full details of this pyroelectric detector and the characteristics of the CNT coating can be found elsewhere.<sup>6</sup>

## 2. Theory

Several papers have presented models for studying the optical properties of CNTs including an effective-

---

E. Theocharous (e.theo@npl.co.uk) is with the Optical Radiation Team, Quality of Life Division, National Physical Laboratory, TW11 0LW, UK. R. Deshpande and A. C. Dillon are with the Hydrogen Storage Group, National Renewable Energy Laboratory, 1617 Cole Boulevard, Golden, Colorado 80401-3393. J. Lehman is with the Sources, Detectors and Displays Group, Optoelectronics Division, National Institute of Standards and Technology, 325 Broadway, Boulder, Colorado 80305.

Received 2 June 2005; revised 19 September 2005; accepted 20 September 2005.

0003-6935/06/061093-05\$15.00/0

© 2006 Optical Society of America

medium approximation that uses the Maxwell-Garnett theory<sup>7</sup> (MGT) and more recently a semianalytical method.<sup>8</sup> From these models it is apparent that some variation in the absorption efficiency is expected but that one may optimize this efficiency for a wavelength range by varying the tube topology.

The dielectric function for well-aligned carbon nanotubes is constructed based on the topology of aligned cylinders oriented perpendicularly to the detector surface and on the dielectric constants for graphite. Our measurements of responsivity are based on an optical beam propagating along the tube axis; thus in the MGT formulation the electric field is perpendicular to the tube axis. García-Vidal *et al.*<sup>7</sup> expressed the dielectric function for this orientation as

$$\epsilon^p = \frac{\epsilon_{\parallel}(\omega) + \Delta + f[\epsilon_{\parallel}(\omega) - \Delta]}{\epsilon_{\parallel}(\omega) + \Delta - f[\epsilon_{\parallel}(\omega) - \Delta]}, \quad (1)$$

where the fill factor is approximated by

$$f \approx \frac{(\pi r_{\text{tube}}^2) n_{\text{tubes}}}{\text{Area}_{\text{detector}}}, \quad (2)$$

and  $\epsilon_{\parallel}$  and  $\epsilon_{\perp}$  are the parallel and perpendicular dielectric functions, respectively, of graphite. For brevity in Eq. (1),

$$\Delta = [\epsilon_{\parallel}(\omega)/\epsilon_{\perp}(\omega)]^{1/2}. \quad (3)$$

Using data for graphite that are available in the *Handbook of Optical Constants of Solids II*,<sup>9</sup> we calculated dielectric function  $\epsilon^p$  and the corresponding index  $n = \sqrt{\epsilon^p}$ . From this, the detector absorption efficiency can be approximated by the use of Fresnel equations.

For analysis, CNT cylinders 30  $\mu\text{m}$  long and 10 nm in diameter deposited onto a nickel electrode on the LiNbO<sub>3</sub> pyroelectric plate are considered. This analysis is an objective basis for estimating detector efficiency as a function of wavelength based on CNT topology. From qualitative examination of the coating by a representative scanning-electron microscope image shown in Fig. 1, it is known that these MWNTs are not perfectly aligned cylinders.

For the sake of discussion, the absorption efficiency at a single wavelength near 11  $\mu\text{m}$  can be calculated, based on the MGT, for fill factors ranging from 0.1 to 0.9. This range corresponds to cylinder gaps from 3 diameters to direct contact. The calculation indicates that a larger fill factor (greater tube spacing) corresponds to lower absorption efficiency. However, considering the entire range of fill factors as shown in Fig. 2, the condition of tubes touching is also undesirable. There are other considerations beyond this analysis. By repeating the analysis, it may be shown that the optimum spacing is wavelength dependent. Thus, for a detector that has a broad and uniform

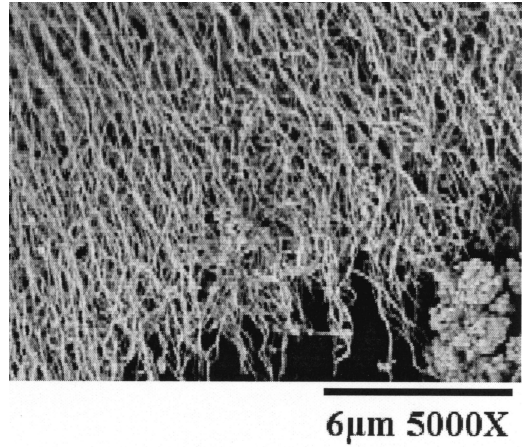


Fig. 1. Scanning-electron microscope image of the MWNT coating. Note that the tubes are not perfectly aligned, as idealized in the MGT model.

spectral responsivity, a range of tube spacings is desirable. The results in Fig. 2 also indicate that it might be impossible to achieve a coating absorption efficiency greater than 90%. In this case the actual topology of the MWNT coating, rather than idealized topology, is probably preferred but more difficult to model and defend on a rigorous basis. For example, long crooked tubes that are poorly aligned are probably advantageous to enhance scattering among the tubes, thus providing multiple opportunities for photons to be absorbed.

### 3. Detector Fabrication

We consider this study to be a continuation of a proof of principle proposed earlier, and the details of the detector preparation are discussed elsewhere.<sup>6</sup> For continuity it is important to consider several points. Arguably, lithium tantalate (LiTaO<sub>3</sub>) is preferable to LiNbO<sub>3</sub> for our application because the its pyroelectric coefficient is nearly two times greater.<sup>10,11</sup> The Curie temperature for LiTaO<sub>3</sub> is low (660 °C), approaching that of the furnace temperature during

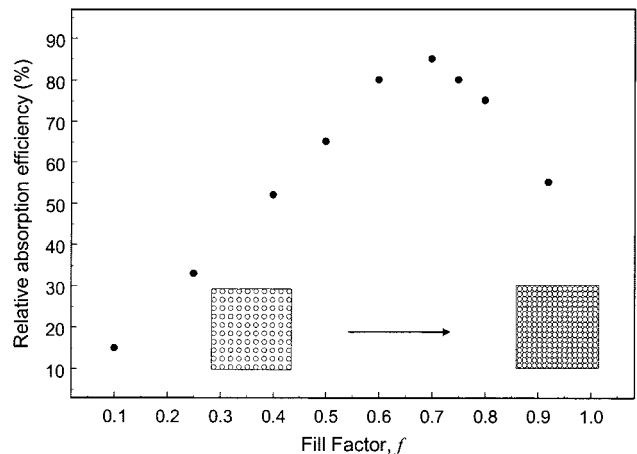


Fig. 2. Calculation of detector absorption efficiency based on Eq. (1).

processing, while the Curie temperature of  $\text{LiNbO}_3$  is approximately  $1200^\circ\text{C}$ .<sup>12</sup> Hot-wire chemical vapor deposition requires relatively high temperatures, reducing atmospheres, and the presence of metal catalysts on the crystal surface, which, as we have observed, can undesirably increase the electrical conductivity and possibly change the spontaneous polarization of the crystal. It is well known that the sensitivity of any thermal detector is inversely related to the detector's thermal mass.<sup>13</sup> We know that, all other things being equal, thinner pyroelectric detectors are more sensitive.<sup>14</sup> This principle must be optimized along with the more subjective and practical consideration that extremely thin detector crystals are difficult to work with experimentally. In the future we expect that our processing will be adapted and refined to accommodate thinner samples of  $\text{LiTaO}_3$  and other thermal detector platforms.

#### 4. Detector Characterization Facilities and Method

The performance of the MWNT pyroelectric detector was characterized by use of the National Physical Laboratory (NPL) infrared detector characterization facilities.<sup>15</sup> The NPL infrared spectral responsivity measurement facility is based on a double-grating monochromator of 0.25 m focal length operating in the subtractive mode. Full details on this facility can be found elsewhere.<sup>16</sup> For further information on the NPL spatial uniformity of response measurement facility and the NPL linearity of response measurement facility the reader is referred to Refs. 15 and 17, respectively. The maximum level of spectral irradiance at which linearity was measured was restricted by the maximum spectral radiance available from the 2 mm wide element of the tungsten strip lamp. During the linearity characterization, the unfiltered output of a tungsten strip lamp with a silica window was used. This was deemed acceptable because of the spectral flatness of the spectral responsivity of the CNT pyroelectric detector (see Subsection 5.A below).

For all the radiometric evaluations described in this paper, the MWNT pyroelectric detector was used in combination with a transimpedance amplifier operated at a fixed gain of  $10^8 \text{ V A}^{-1}$ . All measurements presented in this paper were performed at a modulation frequency of 70 Hz.

#### 5. Results

##### A. Measurements of the Relative Spectral Responsivity and Specific Detectivity

Figure 3 shows the relative spectral responsivity of the CNT pyroelectric detector in the wavelength range  $0.9\text{--}14 \mu\text{m}$ , normalized at  $1.6 \mu\text{m}$ . The error bars shown in Fig. 3 represent the  $1\sigma$  uncertainty of the measurements. The plot shows that the relative spectral responsivity was approximately flat in the wavelength range  $1.6\text{--}14.0 \mu\text{m}$ . This, in turn, means that the absorptivity of the MWNT coating was also flat because that is the main parameter that governs the relative spectral responsivity of thermal detectors.<sup>1</sup> For wavelengths below  $1.6 \mu\text{m}$  the response of

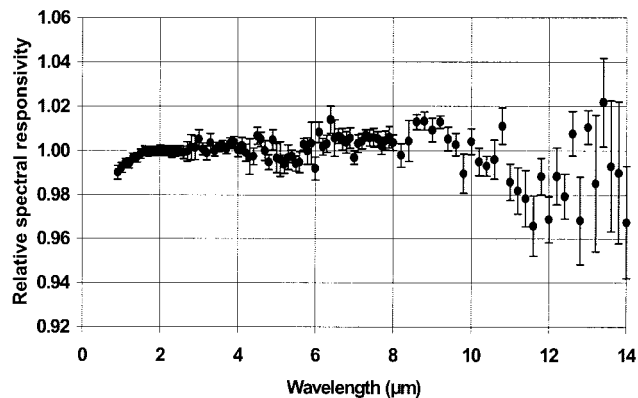


Fig. 3. Relative spectral responsivity of the MWNT pyroelectric detector normalized at  $1.6 \mu\text{m}$ . Error bars represent the  $1\sigma$  uncertainty of the measurements.

the detector decreased monotonically with wavelength to  $0.9 \mu\text{m}$ , the shortest wavelength studied. This behavior confirms data previously reported by Lehman *et al.*<sup>6</sup> A similar behavior was also observed in some other good-quality metal-black coatings such as silver-black and some gold-black coatings. No measurements were attempted for wavelengths longer than  $14 \mu\text{m}$  because the signal-to-noise ratio of the measurements was extremely poor owing to the poor noise equivalent power of the detector and the low radiant power coming through the double-grating monochromator.

The dc equivalent absolute spectral responsivity of the MWNT pyroelectric detector in combination with the transimpedance amplifier with  $10^8 \text{ V/A}$  gain at  $1.6 \mu\text{m}$  for a 70 Hz modulation frequency was measured by comparison with NPL standards to be  $9.03 \text{ V W}^{-1}$ . The noise power spectral density of the detector-amplifier combination at 70 Hz was measured to be  $1.46 \mu\text{V Hz}^{-1/2}$ . Ignoring the noise contribution that is due to the transimpedance amplifier (the noise was dominated by the pyroelectric detector), we estimated the specific detectivity ( $D^*$ ) of the CNT pyroelectric detector at  $1.6 \mu\text{m}$  and 70 Hz to be  $1.82 \times 10^6 \text{ cm Hz}^{1/2} \text{ W}^{-1}$ . This is a relatively poor value compared with that of gold-black-coated  $\text{LiTO}_3$  pyroelectric detectors, which have  $D^*$  values typically 2 orders of magnitude higher. The low  $D^*$  value of the MWNT pyroelectric detector was not unexpected because this detector was based on a  $\text{LiNbO}_3$  crystal  $250 \mu\text{m}$  thick. The thicker crystal (typically a factor of 5 thicker than  $\text{LiTO}_3$  pyroelectric detectors studied previously), in combination with the poorer pyroelectric characteristics of the  $\text{LiNbO}_3$  crystal, can account for most of the observed difference. Furthermore, the coating deposition required the  $\text{LiNbO}_3$  crystal to be heated to temperatures in excess of  $300^\circ\text{C}$ ,<sup>6</sup> which may also have led to a deterioration of the crystal's pyroelectric properties.

##### B. Temperature Coefficient of Response

We obtained the temperature coefficient of response by measuring the responsivity of the detector at a

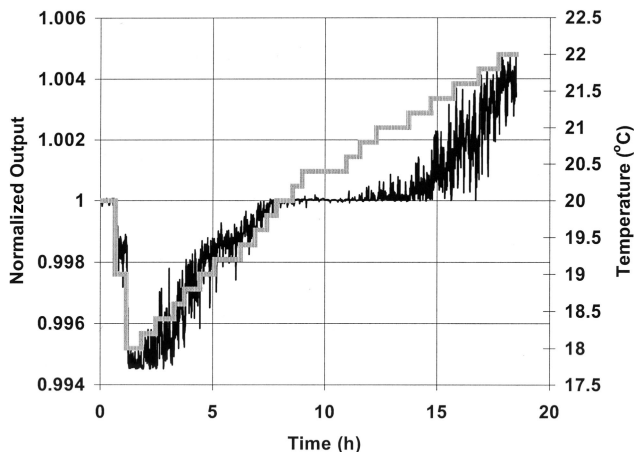


Fig. 4. Normalized output of the MWNT pyroelectric detector while its temperature (the lighter curve) was decreased from 20 °C to 18 °C and then increased to 22 °C.

number of temperatures in the 20 °C–30 °C temperature range. The temperature coefficient is derived from the slope of the plot of detector responsivity versus temperature. Unlike for other detectors examined, the plot of detector responsivity versus temperature of the MWNT pyroelectric detector deviated severely from linearity. Furthermore, the drift characteristics of the detector depended strongly on temperature. Figure 4 shows the normalized output of the MWNT pyroelectric detector when it was illuminated with pseudomonochromatic (FWHM bandwidth, 25 nm) radiation of 1.6  $\mu\text{m}$  peak wavelength over a period of  $\sim 18$  h. During this time the temperature of the detector (shown by the lighter curve in the same plot) was reduced from 20 °C to 18 °C and then increased to 22 °C. Two effects were immediately obvious. First, the temperature coefficient of the response was highest near 18 °C and 22 °C but was low near 20.5 °C. Second, the scatter of successive measurements of the detector output is highest near 18 °C and 22 °C but is lowest near 20.5 °C. The authors can only assign this behavior to stresses in the pyroelectric crystal owing to thermal expansion at different temperatures. The temperatures at which noise minima occur are reproducible and could potentially be utilized to enhance detector performance.

### C. Spatial Uniformity of Response

Figure 5 shows the normalized response of the MWNT pyroelectric detector measured at several points on the active area of this detector by use of a spot 0.4 mm in diameter. The largest deviation from the maximum response is less than 3%, which is typical for pyroelectric detectors of this size.<sup>3</sup> It has been found that the spatial nonuniformity of the response of a pyroelectric detector can arise from the pyroelectric crystal itself (e.g., from thickness variations)<sup>18</sup> or from the spatial variations of the quality of the black coating. Unambiguous identification of the origin of the spatial nonuniformity would require the

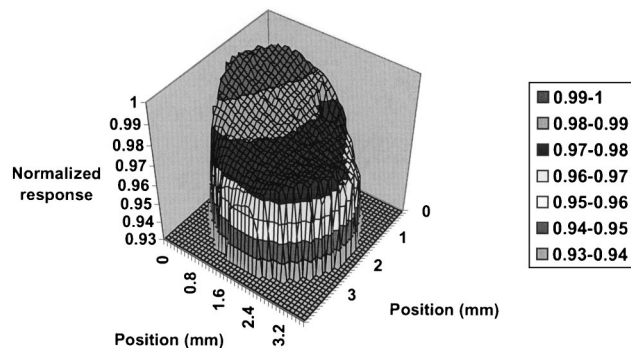


Fig. 5. Spatial uniformity of the response of the MWNT pyroelectric detector.

removal of the MWNT coating, something that the authors were reluctant to do because of the rarity of this detector.

### D. Linearity Characteristics

Figure 6 shows the linearity factor<sup>17</sup> of the MWNT pyroelectric detector–amplifier combination. The abscissa represents the dc equivalent radiant power incident in the 2 mm diameter spot on the active area of the detector illuminated by the incident radiation. Error bars represent the standard deviation of eight measurements of the linearity factor at each value of radiant power. Data shown in Fig. 6 indicate no measurable deviation from linearity in the 0.06–2.8 mW radiant power range.

### E. Stability

Figure 7 shows the normalized response of the MWNT pyroelectric detector over a 48 h period. No active temperature stabilization was utilized during these measurements. A platinum-black-coated  $\text{LiTiO}_3$  detector was used as a reference detector during this stability test. The unfiltered output of a tungsten strip lamp with a 2 mm wide tungsten element and a silica window was used to illuminate a 2 mm diameter spot on the active areas of both detectors. During the period of this test, the output of both detectors exhibited identical drifts of as much as 0.6%. These drifts were assigned to drifts in the lamp output be-

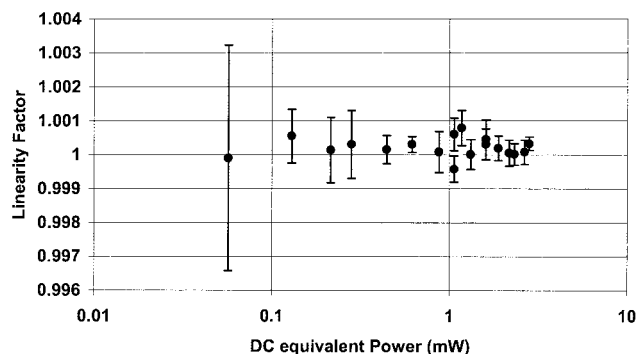


Fig. 6. Linearity characteristics of the MWNT pyroelectric detector. Error bars represent the standard deviation of eight measurements of the linearity factor at each value of radiant power.

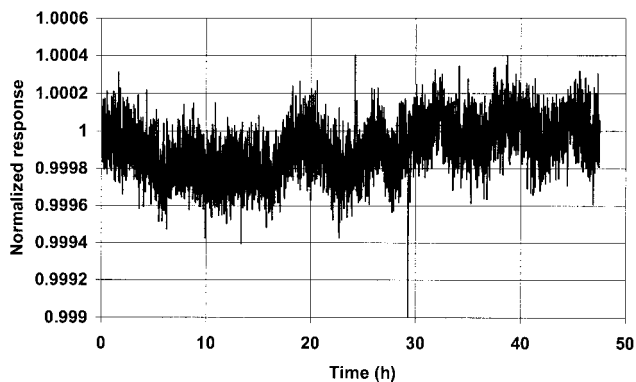


Fig. 7. Normalized response of the MWNT pyroelectric detector during 48 h.

cause they were common to the outputs of both detectors.

## 6. Conclusions

The performance of a pyroelectric detector with a multiwalled carbon nanotube coating was evaluated in the 0.9–14  $\mu\text{m}$  wavelength range. The relative spectral responsivity of this detector was shown to be spectrally invariant over most of the wavelength range examined and was shown to be comparable (in terms of spectral neutrality) to the best infrared black coatings currently available. This result is promising because black coatings with spectrally flat absorbance profiles are usually associated with the highest absorbance values.<sup>19</sup> Theory predicts that the absorbance of MWNT coatings will depend on the fill factor and will exhibit some dependency on wavelength. The results of this study show that the relative spectral responsivity of the MWNT-coated pyroelectric detector and therefore the absorbance of the MWNT coating does not exhibit any wavelength dependency in the 1.6–14  $\mu\text{m}$  wavelength range. This observation can be explained only by the CNTs' being long and crooked as well as being poorly aligned. This conclusion is supported by the shape of the nanotubes recorded by scanning-electron microscopy and shown in Fig. 1. The performance of this detector (in terms of noise equivalent power and specific detectivity) was limited by the very thick (250  $\mu\text{m}$ )  $\text{LiNbO}_3$  pyroelectric crystal onto which the coating was deposited. The detector was shown to be linear in the 0.06–2.8 mW radiant power range, and its spatial uniformity of response was similar to that of other pyroelectric detectors that use different types of black coating. The MWNT coating was reported to be much more durable than other infrared black coatings commonly used to coat thermal detectors in the infrared, such as metal blacks. This property, in combination with its demonstrated excellent spectral flatness, suggests that this coating appears extremely promising for thermal detection applications in the infrared.

This paper is published with the permission of the Controller of Her Majesty's Stationery Office and the

Queen's Printer for Scotland and supported by the National Measurement System Policy Unit of the Department of Trade and Industry (UK).

## References

1. W. R. Blevin and J. Geist, "Influence of black coatings on pyroelectric detectors," *Appl. Opt.* **13**, 1171–1178 (1974).
2. D. J. Advena, V. T. Bly, and J. T. Cox, "Deposition and characterization of far-infrared absorbing gold black films," *Appl. Opt.* **32**, 1136–1144 (1993).
3. J. Lehman, E. Theocharous, G. Eppeldauer, and C. Pannel, "Gold-black coatings for freestanding pyroelectric detectors," *Meas. Sci. Technol.* **14**, 916–922 (2003).
4. R. Saito, G. Dresselhaus, and M. S. Dresselhaus, *Physical Properties of Carbon Nanotubes* (Imperial College Press, London, 2003), p. 212.
5. J. H. Lehman, C. Engrakul, T. Gennet, and A. C. Dillon, "Single-wall carbon nanotube coating on a pyroelectric detector," *Appl. Opt.* **44**, 483–488 (2005).
6. J. H. Lehman, R. Deshpande, P. Rice, and A. C. Dillon, "Carbon multi-walled nanotubes grown by HWCVD on a pyroelectric detector," *Infrared Phys. Technol.* (to be published).
7. F. J. García-Vidal, J. M. Pitarke, and J. B. Pendry, "Effective medium theory of the optical properties of aligned carbon nanotubes," *Phys. Rev. Lett.* **78**, 4289–4292 (1997).
8. X. H. Wu, L. S. Pan, X. J. Fan, D. Xu, H. Li, and C. X. Zhang, "A semi-analytic method for studying optical properties of aligned carbon nanotubes," *Nanotechnology* **14**, 1180–1186 (2003).
9. A. Borghesi and G. Guizzetti, "Graphite (C)," in *Handbook of Optical Constants of Solids II*, E. Palik, ed. (Academic, 1991), pp. 449–460.
10. A. M. Glass, "Ferroelectric  $\text{Sr}_{1-x}\text{Ba}_x\text{Nb}_2\text{O}_6$  as a fast and sensitive detector of infrared radiation," *Appl. Phys. Lett.* **13**, 147–148 (1968).
11. R. L. Byer and C. B. Roundy, "Pyroelectric coefficient direct measurement technique and application to a nsec response time detector," *Ferroelectrics* **3**, 333–338 (1972).
12. K. Nassau, H. J. Levinstein, and G. M. Loiacono, "Ferroelectric lithium niobate. 2. Preparation of single domain crystals," *J. Phys. Chem. Solids* **27**, 989–996 (1966).
13. W. Budde, *Physical Detectors of Optical Radiation*, Vol. 4 of *Optical Radiation Measurements*, F. Grum and C. J. Bartleson, eds. (Academic, 1983), p. 130.
14. J. H. Lehman, A. M. Radojevic, R. M. Osgood, Jr., and M. Levy, "Fabrication and evaluation of a freestanding pyroelectric detector made from single-crystal  $\text{LiNbO}_3$  film," *Opt. Lett.* **25**, 1657–1659 (2000).
15. E. Theocharous, F. J. J. Clarke, L. J. Rodgers, and N. P. Fox, "Latest techniques at NPL for the characterisation of infrared detectors and materials," in *Materials for Infrared Detectors III*, R. E. Longshore and S. Sivananthan, eds., *Proc. SPIE* **5209**, 228–239 (2003).
16. E. Theocharous, J. Ishii, and N. P. Fox, "A comparison of the performance of a photovoltaic  $\text{HgCdTe}$  detector with that of a large area single pixel QWIP for infrared radiometric applications," *Infrared Sci. Technol.* **46**, 309–322 (2004).
17. E. Theocharous, J. Ishii, and N. P. Fox, "Absolute linearity measurements on  $\text{HgCdTe}$  detectors in the infrared," *Appl. Opt.* **43**, 4182–4188 (2004).
18. E. Theocharous, N. P. Fox, and T. R. Prior, "A comparison of the performance of infrared detectors for radiometric applications," in *Optical Radiation Measurements III*, J. M. Palmer, ed., *Proc. SPIE* **2815**, 56–69 (1996).
19. N. Nelms and J. Dawson, "Goldblack coating for thermal infrared detectors," *Sensors Actuators A* **120**, 403–407 (2005).